Materials and Structures/Matériaux et Constructions, Vol. **29**, June 1996, pp 259-266

SCIENTIFIC REPORTS

Size effects on concrete fracture energy: dimensional transition from order to disorder

Alberto Carpinteri and Bernardino Chiaia

Department of Structural Engineering, Politecnico di Torino, 10129 Torino, Italy

ABSTRACT

The nominal fracture energy of concrete structures is constant for relatively large structures, whereas it increases with size for relatively small structures. If the energy dissipation space is modeled as a monofractal domain, with a non-integer dimension comprised between 2 and 3, a unique slope in the bilogarithmic fracture energy versus size diagram is found, as was stated in a previous paper [1]. On the other hand, when the scale range extends over more than one order of magnitude, a continuous transition from slope + 1/2 to zero slope may appear, according to the hypothesis of multifractality of the fracture surface [1]. This means that, at small scales, a Brownian microscopic disorder is prevalent whereas, at large scales, the effect of disorder vanishes, yielding a macroscopical homogeneous behavior. The dimensional transition from disorder to order may be synthesized by a Multifractal Scaling Law (MFSL) valid for toughness, in perfect correspondence with the MFSL valid for strength, which has been described in a previous paper [2]. The MFSL for fracture energy is applied, as a best-fitting method, to relevant experimental results in the literature, allowing for the extrapolation of fracture energy values valid for real-sized structures.

RÉSUMÉ

*L'énergie de fracture nominale des structures en béton est constante pour des structures relativement grandes, alors qu'elle augmente avec les dimensions pour les structures relativement petites. Si l'espace de dissipation de l'énergie est modelé comme domaine monofractal avec une dimension non-intégrale comprise entre deux et trois, on observe une seule pente dans le diagramme bilogarithmique énergie de fracture-dimensions, comme il a déjà été observé dans un article précédent [1]. D'autre part, si l'intervalle d'échelle s'étend à plus d'un ordre de grandeur, une transition continue de la pente + 1/2 à la pente zéro peut apparaître, en accord avec l'hypothèse de multifractalité de la surface de fracture [1]. Cela montre qu'un désordre microscopique Brownien prédomine dans les petites échelles, alors que, dans les grandes, l'effet de désordre disparaît et donne lieu à un comportement macroscopique homogène. La transition dimensionnelle du désordre à l'ordre peut être synthétisée par la Loi d'Échelle Multifractale (MFSL) valable pour la ténacité, en parfait accord avec la Loi d'Échelle Multifractale valable pour la résistance, qui a été décrite dans un article précédent [2]. La Loi d'Échelle Multifractale pour l'énergie de fracture est appliquée, comme méthode d'interpolation «*best-fitting*», aux résultats d'expérimentation plus importants contenus dans la littérature, car elle permet d'extrapoler les valeurs de l'énergie de fracture valables pour les structures de dimensions réelles.*

1. RILEM DEFINITION OF FRACTURE ENERGY

The constitutive model that appears more suitable for describing the mechanical behavior of "quasi-brittle" materials like concrete, ceramics and rocks is the Cohesive Crack Model [3], which is based on two distinct relationships (Fig. 1). The first one is the elastic-plastic stress-strain law, holding up to the ultimate tensile stress σ_u, and the second is a stress-crack opening displacement law, also called the cohesive law, which describes the softening behavior provided by the damaged process zone.

The area under the cohesive law $\sigma(w)$ represents the energy dissipated on the unitary crack surface and, by definition, is called the fracture energy $\mathcal{G}_F$ of the material:

$$\mathcal{G}_F = W_F / A_{lig} \quad (1)$$

where W_F is the total work necessary for the complete fracture of the specimen and A_{lig} is the area of the initial resisting ligament.

The cohesive law is generally assumed as a material

Editorial note

Prof. Alberto Carpinteri and Dr. Bernardino Chiaia are both working at the Politecnico di Torino, a RILEM Titular Member. Prof. Carpinteri is involved in the work of RILEM Technical Committees 147-FMB on Fracture Mechanics applications to anchorage and Bond and 148-SSC on Tests methods for the Strain Softening response on Concrete. In 1982, Prof. Alberto Carpinteri was awarded the Robert L'Hermite Medal for his outstanding research work.

0025-5432/96

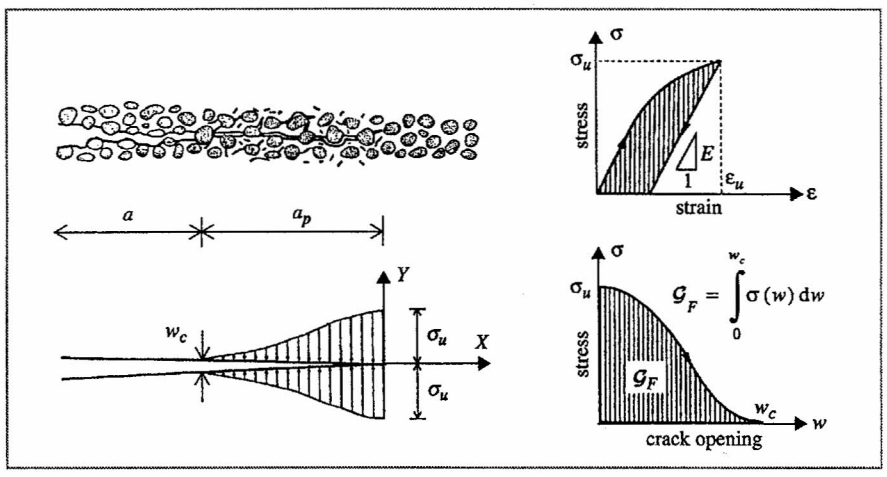

Fig. 1 – Cohesive Crack Model [3].

characteristic, since it intimately depends on the material microstructure and on the dissipation mechanisms involved in the fracture process (bridging, creep, aggregate interlocking, etc.); therefore, the fracture energy $\mathcal{G}_F$ is usually considered as a material constant.

Starting from its definition, the fracture energy $\mathcal{G}_F$ does not represent a local toughness parameter, like the critical stress-intensity factor K_{IC} (tensional fracture toughness); it rather represents a mean-field parameter, involving the whole complexity of microscopical phenomena ahead of the crack tip, which take part in the total work-of-fracture (energy fracture toughness). The great advantage of such a global parameter is provided by the absence of linearity requirements in the fracture process: no information on the singular stress field at the crack tip is needed, and Linear Elastic Fracture Mechanics can be neglected. On the other hand, the physical meaning of $\mathcal{G}_F$ proves to be ambiguous since it has been defined, according to equation (1), as purely a surface energy ($[F][L]^{-1}$). On the contrary, it refers to a much more complicated process of dissipation, taking place in a higher dimensional space which includes all the previously mentioned micromechanisms of damage [1].

2. SIZE EFFECTS ON RILEM FRACTURE ENERGY

The experimental determination of concrete fracture energy $\mathcal{G}_F$ is nowadays governed by a RILEM Recommendation [4] and consists of a standard displacement-controlled three-point bending test. A huge number of tests preceded and followed the publication of the aforementioned Recommendation: unfortunately, the increase of the measured value of $\mathcal{G}_F$ has always been detected with increasing specimen size, which is essentially the same trend observed in the case of other toughness parameters (K_{IC} or *J-integral*), even in different materials. In the first extensive round-robin, almost 700 beams were tested in 14 different laboratories, but the size range was rather small [5]; after analyzing the results, Hillerborg concluded that $\mathcal{G}_F$ could be considered as a material constant, since its variation with size was less than one-third of the corresponding variation of strength. Subsequent investigations on wider size ranges [6] showed that the $\mathcal{G}_F$ variation with size is not at all negligible, and that this scaling effect has to be considered together with the more familiar size effect on tensile strength [2].

A well-known interpretation of this scaling behavior is owed to Wittmann *et al.* [7, 8]. They state that the increase with size of the fracture process zone (FPZ) width a_p is responsible for the variation of the nominal fracture energy $\mathcal{G}_F$, which causes an increase of the critical crack opening displacement $w_2 = w_c$ in a bilinear cohesive law (Fig. 2). Since the energy dissipation takes place in the fracture process zone, whose width expands during crack propagation (R-curve behavior) at least up to a limit value $(w_2)_{lim}$ (fully-developed process zone), it is reasonable to suppose that in larger specimens, where the FPZ can develop entirely, a higher value of w_c is reached, thereby yielding a higher measured fracture energy. The authors propose a local fracture energy $g_F(x)$, proportional to the FPZ width and thus to w_c, whose integration along the fracture path provides a size-dependent fracture energy, in accordance with the experimental values. Beyond a well-defined structural

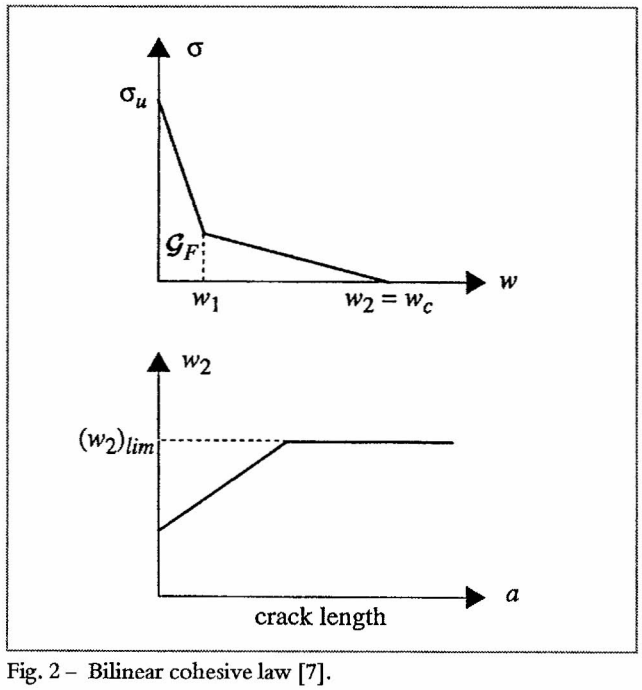

Fig. 2 – Bilinear cohesive law [7].

size, the FPZ attains its highest width and remains constant; therefore, an asymptotic value of $\mathcal{G}_F$ is measured in the limit of the largest sizes.

Mai and Cotterell [9] proposed a bilinear size-effect law for fracture energy, based on several investigations of different materials characterized by well-defined process zones:

$$\mathcal{G}_F = \mathcal{G}_e + Cb \quad (b < b^*) \tag{2a}$$

$$\mathcal{G}_F = \mathcal{G}_F^{\infty} \quad (b > b^*) \tag{2b}$$

where b^* is a threshold size, $\mathcal{G}_e$ is the "essential work of fracture", C and $\mathcal{G}_F^{\infty}$ are two constants to be determined from the tests, with the latter being the asymptotic value of fracture energy valid for the largest sizes. An application of equations (2) is shown in Fig. 3.

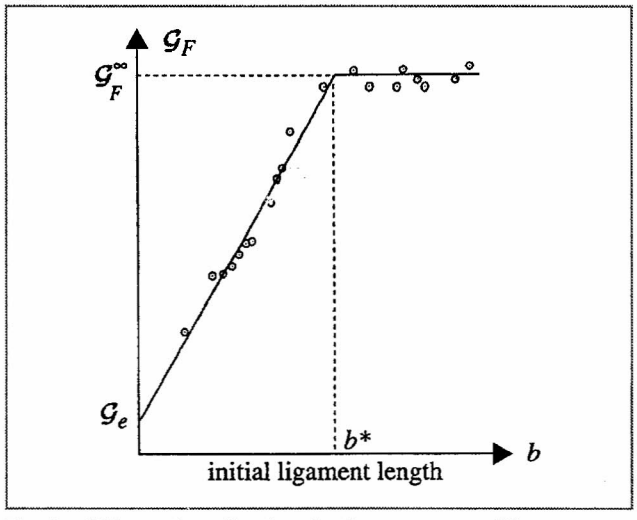

Fig. 3 – Bilinear size effect law for fracture energy [9].

An extensive investigation on the fracture energy size effect has been reported by Elices *et al.* [10-12]. Three causes, not adequately taken into account by the RILEM test, are considered to be responsible for the variation of toughness with size: the energy dissipation from hysteresis in the testing equipment and in the lateral supports, the bulk dissipation in the most stressed regions of the sample and the dissipated energy at the end of the loading process, which is neglected due to the cutting of the P-δ tail. It can be argued that this analysis, although pointing out some remarkable details of the RILEM test, does not focus on the intimate nature of the localized energy dissipation, which seems mainly to control the phenomenon.

Other models, alternative to the RILEM definition, have been proposed by Bažant and Kazemi [13], based on the Size Effect Law for strength [14] and on the R-curve concept, by Karihaloo and Nallathambi [15], based on the "Effective Crack Model", and by Jenq and Shah [16], based on the "Two-Parameter Fracture Model". Although they all show less sensitivity to the size effect with respect to the RILEM fracture energy definition, they represent less significant models from a physical point of view.

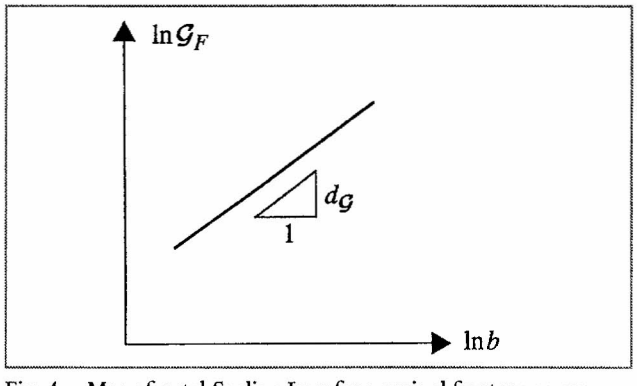

Fig. 4 – Monofractal Scaling Law for nominal fracture energy.

3. MULTIFRACTAL SCALING LAW FOR FRACTURE ENERGY

As stated in a previous paper [1], the complexity of the energy dissipation during a fracture process can be consistently synthesized by considering this dissipation occurring in a domain with a fractional topological dimension comprised between 2 and 3. By applying a real-space renormalization procedure, the scaling behavior of the nominal fracture energy $\mathcal{G}_F$ can be described, in the bilogarithmic diagram, as follows:

$$\ln\mathcal{G}_F = \ln\mathcal{G}_F^{\star} + d_{\mathcal{G}}\ln b \tag{3}$$

where b is a characteristic structural size, $d_{\mathcal{G}}$ is the fractional topological increment, due to disorder, of the energy dissipation space and $\mathcal{G}_F^{\star}$ is the renormalized fracture energy, whose anomalous physical dimensions $([F][L]^{-(1+d_{\mathcal{G}})})$ imply that the energy dissipation is, in some way, intermediate between a purely surface dissipation (which is the RILEM hypothesis) and a bulk dissipation (which is the classical approach of Limit Analysis and Damage Mechanics theories).

In any case, the monofractal scaling behavior described by equation (3) and showed in Fig. 4 does not adequately reproduce the experimental results, since an infinite nominal fracture energy would be predicted for the largest sizes by equation (3), though an asymptotic constant value of $\mathcal{G}_F$ has always been detected by the tests. Moreover, the topology of the fracture surfaces appears experimentally multifractal [1] in the sense that, as in any natural fractal set, the presence of an internal microstructural scale l_{ch} and of an external macrostructural size b provides the progressively-decreasing influence of disorder when increasing the scale of observation. From the mechanical point of view, this geometrical trend implies that the effect of microstructural disorder on the mechanical properties of the material becomes progressively less important for the larger specimens, whereas it represents the fundamental parameter at the smaller scales [17, 18].

A transition from a disordered (fractal) regime to an ordered (homogeneous) one can therefore be emphasized in the scaling behavior of any mechanical quantity. In the case of fracture energy, the former regime is ideally bounded by a "Brownian" microscopic disorder, corresponding to the highest possible disorder of the fracture domain (local fractal dimension = 2.5), whilst the latter corresponds

to the vanishing of fractality or, equivalently, to the macroscopic homogenization of the microstructure ($d_\mathcal{G} \to 0$) [1]. A strong scale effect is provided by the influence of disorder below the transition scale l_{ch}, whereas beyond l_{ch}, the size effect rapidly vanishes, and the classical Euclidean theories (RILEM approach) become applicable since a constant value of the mechanical quantity is attained.

On the basis of these hypotheses, a Multifractal Scaling Law (MFSL) can be deduced for the nominal fracture energy $\mathcal{G}_F$, in perfect correspondence with the MFSL proposed for the nominal tensile strength [2]. The analytical expression for this Multifractal Scaling Law, represented in Fig. 5, is the following:

$$\mathcal{G}_F(b) = \mathcal{G}_F^{\infty}\left[1 + \frac{l_{ch}}{b}\right]^{-1/2} \tag{4}$$

where $\mathcal{G}_F^{\infty}$ is the nominal asymptotic fracture energy valid within the limit of infinite structural size ($b \to \infty$). The non-dimensional term in square brackets represents the decrease, due to the disorder, of the nominal fracture energy with respect to the constant asymptotic value. Note that the asymptotic requirements are satisfied by the former expression: if one takes the derivative of equation (4) and takes its limit for $b \to 0^+$, the maximum slope of the size effect law, equal to +1/2 (Brownian disorder), is obtained.

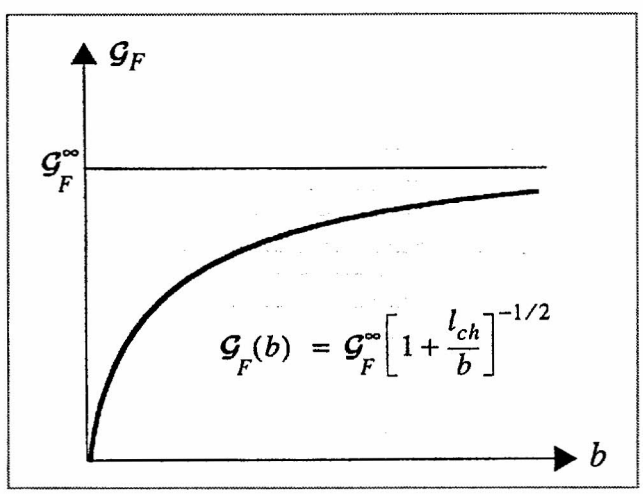

Fig. 5 – Multifractal Scaling Law for nominal fracture energy.

In the bilogarithmic diagram $\ln\mathcal{G}_F$ *vs.* $\ln b$, showed in Fig. 6, the analytical expression becomes:

$$\ln \mathcal{G}_F = \ln \mathcal{G}_F^{\infty} - \frac{1}{2}\ln\left(1 + \frac{l_{ch}}{e^{(\ln b)}}\right) \tag{5}$$

The asymptotes in the bilogarithmic diagram present a peculiar physical meaning. The horizontal asymptote, corresponding to the larger structural sizes, represents the so-called homogeneous regime of the scaling and is described by the following expression:

$$\ln\mathcal{G}_F = \ln\mathcal{G}_F^{\infty} \tag{6}$$

whereas the oblique asymptote, corresponding to the fractal regime of the scaling, is described by:

$$\ln \mathcal{G}_F = \frac{1}{2}\ln b + \ln\left(\frac{\mathcal{G}_F^{\infty}}{\sqrt{l_{ch}}}\right) \tag{7}$$

A very strong difference can be emphasized between the two asymptotes: besides the evident transition in the scaling behavior, they imply different physical mechanisms in the fracture process of the material. Whilst the horizontal asymptote, corresponding to the larger structures, is governed by $\mathcal{G}_F^{\infty}$ which is a purely surface energy, the oblique asymptote, corresponding to the smaller structures, is controlled by the ratio of surface energy to the square root of a length, or, by a stress-intensity factor (K_I) with physical dimensions $[F][L]^{-3/2}$.

On the basis of the MFSL, the RILEM fracture energy, defined as a mean-field quantity, appears to be a physically meaningful parameter only in the homogeneous regime, whereas Linear Elastic Fracture Mechanics, characterized by a local approach (K_I), governs the collapse of unnotched structures only when the characteristic size a of microstructural defects becomes comparable with the macroscopic size b of the specimen or, equivalently, when the influence of disorder becomes essential. Note that this implies a dimensional transition of toughness, which can be reconducted to the non-integer dimensions of the renormalized fracture energy $\mathcal{G}_F^{*}$ [1].

From these considerations, it can be argued that the fundamental Irwin's relation:

$$K_{IC} = \sqrt{\mathcal{G}_{IC} E} \tag{8}$$

relating the critical value of the stress-intensity factor K_{IC}, the fracture energy (or critical value of the energy release rate) $\mathcal{G}_{IC}$ and the elastic modulus E of the material, is valid only for the larger structures when a constant value of fracture energy can be defined. Therefore, on the basis of the MFSL, LEFM always governs the local collapse of a material but can be homogenized into an energy parameter ($\mathcal{G}_F$) only at the larger scales. This is in perfect agreement with the MFSL proposed for tensile strength [2], where the Griffith collapse, valid for the smaller sizes, causes an oblique asymptotic behavior towards infinite values of strength, whereas a constant (minimum) value of strength can be determined for the larger structures.

The intersections of the MFSL and of its asymptotes with the logarithmic axes are reported in Fig. 6; in particular, the intersection Q between the two asymptotes represents a very important point in the diagram. It is characterized, in fact, by a value of the abscissa equal to the characteristic length l_{ch} of the material, which represents a threshold scale between the two different scaling regimes, analogously to the case of the MFSL for tensile strength [2]. This internal length, which is a parameter appearing in any sound modeling approach of heterogeneous materials, is typical of any natural fractal domain, whereas mathematical fractals (monofractals) have no characteristic scale and therefore show a linear and unbounded scaling.

It is reasonable to suppose that the value of l_{ch} is related to the size of heterogeneities in the material microstructure, these being the aggregates in the case of concrete,

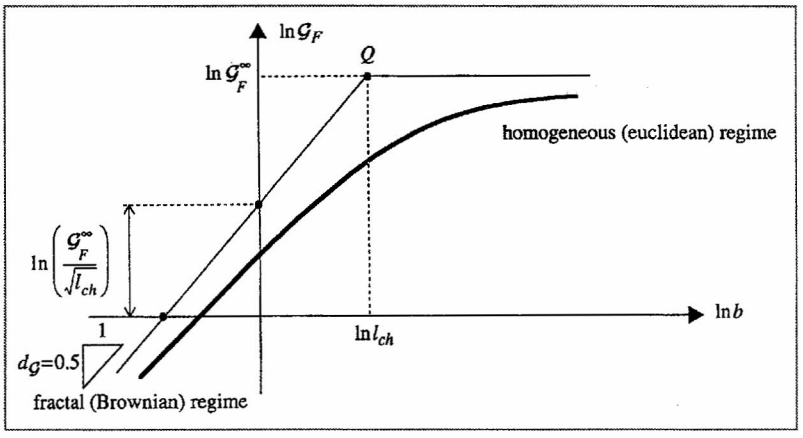

Fig. 6 – Multifractal Scaling Law: bilogarithmic diagram.

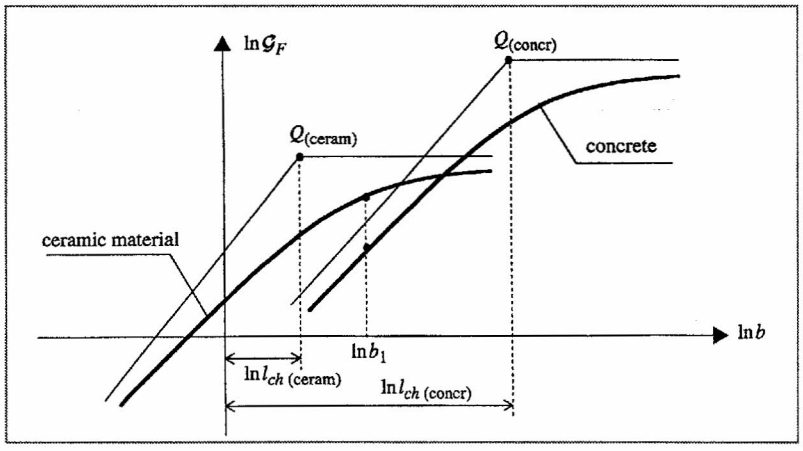

Fig. 7 – Application of the MFSL to two materials with different microstructure.

the grains in the case of metals, the crystals or the pores in the case of rocks, the fibers in a fiber-reinforced composite and even the polymeric chains in a plastic material. In the specific case of concrete, a linear relationship with the maximum aggregate size has been proposed [2]:

$$l_{ch} = \alpha d_{max} \quad (9)$$

The decisive role of the aggregate on the toughness characteristics of concrete is widely recognized nowadays: the measured values of $\mathcal{G}_F$ in the case of mortar are much lower than in the case of concrete [3]; also, clay bricks show a higher toughness if a higher percentage of sand (which represents a large aggregate when compared with clay) is used in the mixture [19].

It can be stated that in the case of a finer-grained material like a ceramic composite, the MFSL is shifted to the left with respect to the case of concrete, with the value of l_{ch} being much lower for ceramics than for concrete (Fig. 7). Therefore, two specimens of different materials, with the same structural dimension b_1, besides obviously showing two different values for the nominal fracture energy, have to be set into two different scaling regimes. With reference to Fig. 7, the concrete specimen behaves according to the fractal regime, whereas the ceramic one lies on the asymptotic branch of the MFSL, thus showing a homogeneous macroscopic behavior.

Generally speaking, one has to determine for each material the proper range of scales where the fractal regime is predominant, and consequently the minimum structural size beyond which the local toughness fluctuations are macroscopically averaged, and a constant value of fracture energy can be assumed.

4. APPLICATION OF THE MFSL TO EXPERIMENTAL DATA

In the present section, the Multifractal Scaling Law is applied in order to interpret the results from experimental tests on different concrete geometries. Two aims are pursued by this statistical analysis: from a physical point of view, the goodness of fit of the size-scale behavior for the nominal fracture energy is provided, whereas from an engineering point of view, the method allows for the extrapolation, from laboratory-sized specimens, of a reliable value of the fracture energy valid for real-sized concrete structures.

A non-linear best-fitting method has been implemented, based on the Levenberg-Marquardt algorithm [20]; in this way, equation (4) is fitted to experimental data, giving as results for the particular concrete mixture and test geometry considered the values $\mathcal{G}_F^\infty$ and l_{ch}. Note that this regression procedure turns out to be more statistically reliable the wider the size range considered in the tests: one order of magnitude of the structural size range should be considered in any case but, unfortunately, this requirement is rarely fulfilled in the literature.

The first geometry to be considered is that of Wittmann *et al.* [7] and consists of a series of compact tests over a size range 1:4 (b_{min} = 150 mm, b_{max} = 600 mm, where b is the initial ligament length). The concrete mixture provides an average compression strength f_c equal to 42.9 MPa, with a maximum aggregate size d_{max} = 16 mm. This test geometry presents the advantage, with respect to the standard RILEM test, of eliminating the specimen's self-weight; nevertheless, it results in being less practical to carry out. Only a two-dimensional similitude is guaranteed, with the thickness t of the specimens being constanly equal to 120 mm. Six specimens have been tested for each representative size. The nominal values of the fracture energy are obtained by the ratio of the total work of fracture (area under the load-displacement curve) to the initial area of the ligament ($b \times t$). Note that the authors cut the end of the softening tail, intending that the hinge-mechanism due to bridging and interlocking between aggregates has not to be taken into account in the toughness evaluation.

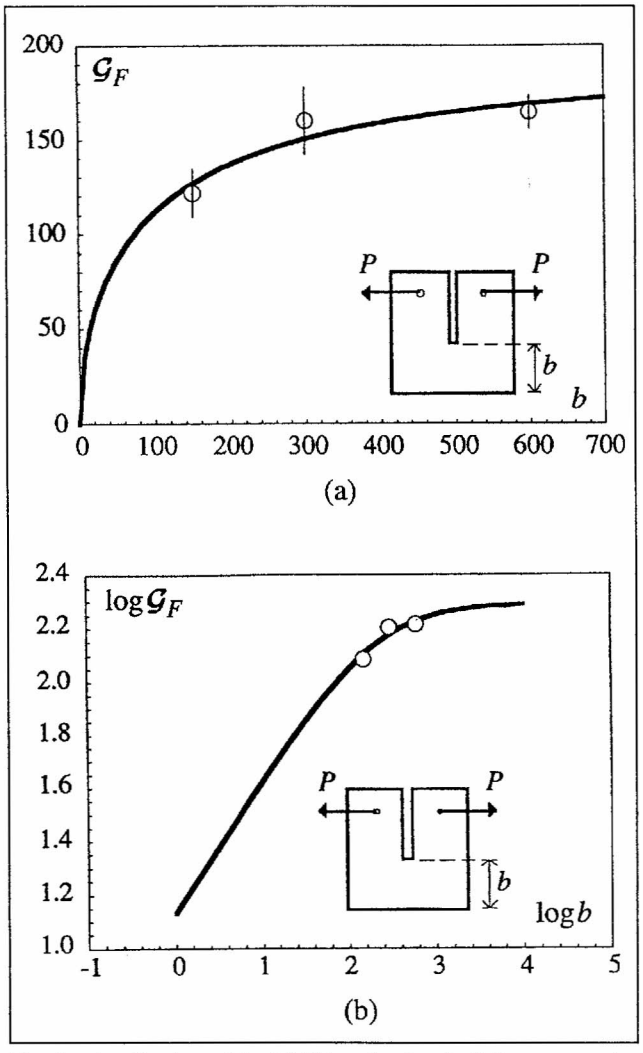

Fig. 8 – Application of the MFSL to the data by Wittmann *et al.* [7]: linear diagram (a), and bilogarithmic diagram (b).

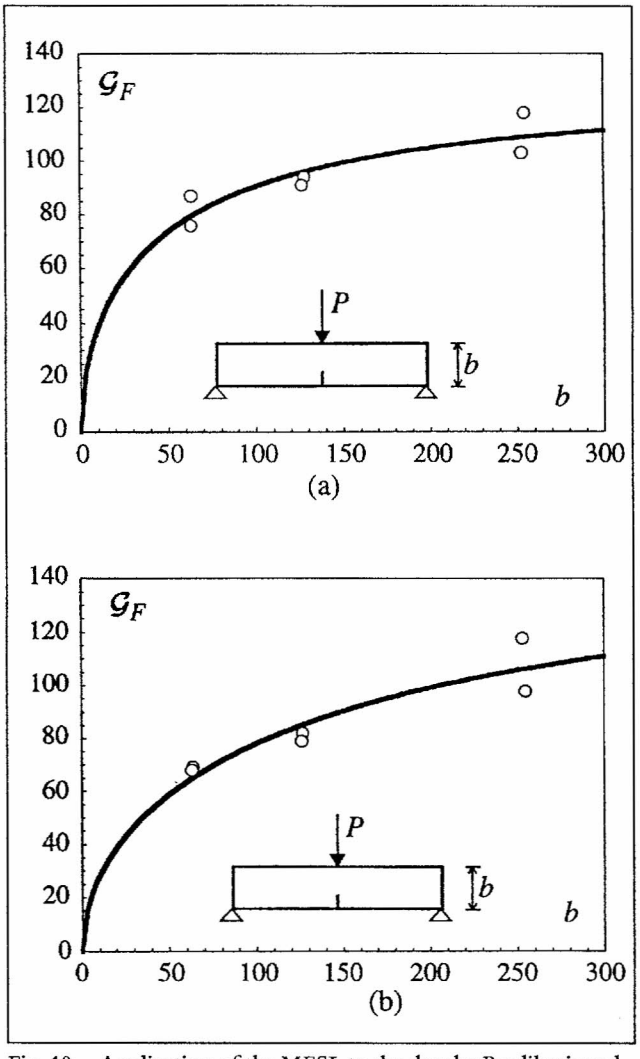

Fig. 10 – Application of the MFSL to the data by Perdikaris and Romeo [21]: Series I (a), and Series II (b).

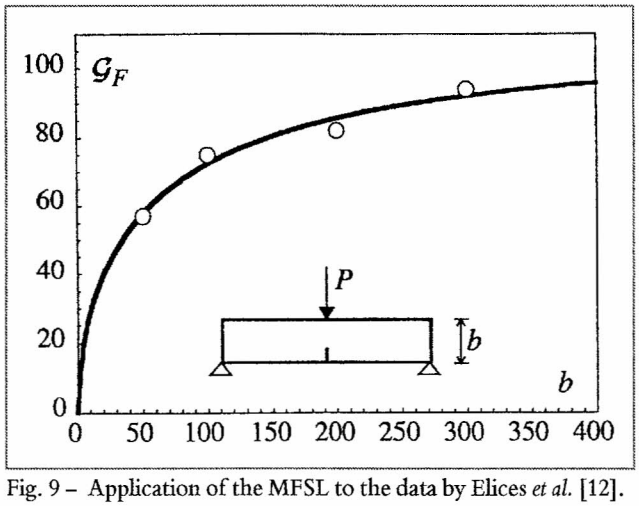

Fig. 9 – Application of the MFSL to the data by Elices *et al.* [12].

The application of the MFSL to the $\mathcal{G}_F$ values is showed in Fig. 8a, whilst the bilogarithmic diagram is represented in Fig. 8b. The asymptotic fracture energy results in $\mathcal{G}_F^{\infty}$ = 196.2 N/m, and the characteristic internal length l_{ch} = 209.5 mm. Therefore, the asymptotic toughness is about 40% larger than the smallest specimen's value (121.5 N/m). Note that by applying the indirect method by Bažant and Kazemi [13], based on the extrapolation from the tensile strength Size Effect Law [14], one would obtain an asymptotic fracture energy equal to 117 N/m, even smaller than the smallest specimen's value! On the basis of equation (9), the non-dimensional parameter α results in $\alpha = l_{ch} / d_{max}$ = 13.1. The correlation coefficient, which is a clue to the goodness of fit, turns out to be R = 0.937.

Experimental results obtained by rigorously following the RILEM Recommendation [4] are those by Elices *et al.* [12]. Three-point bending tests under crack opening control have been carried out by the authors on beams made of concrete with d_{max} = 10 mm and f_c = 33.1 MPa. As in the previous case, only a two-dimensional similitude is provided, with the thickness t being equal to 100 mm for all the beams. The beam height, assumed as the reference size, ranges from 50 mm to 300 mm (range 1:6). The nominal fracture energy is obtained from the total work of fracture (considering also the weight of the beam and of the testing equipment [4]) divided by the initial ligament $((b - a_0) \times t$, where $a_0 = b/3$ is the initial notch depth).

The application of the MFSL is shown in Fig. 9; the best-fitting values are $\mathcal{G}_F^{\infty}$ = 110.6 N/m and l_{ch} = 133.1 mm respectively. The asymptotic fracture energy is therefore almost 90% larger than the smallest specimen's value (57 N/m). The non-dimensional parameter $\alpha = l_{ch}/d_{max}$ is equal to 13.3, whilst the correlation coefficient turns out to be R = 0.982.

Another series of three-point bending tests, carried out according to the RILEM standards, is that of Perdikaris and Romeo [21]. Two mixtures of concrete were examined with the same granulometry (d_{max} = 6.4 mm), but with different compressive strengths. In the case of Series I, a result of f_c(I) = 35 MPa was obtained, whereas in the case of Series II, a higher strength was obtained (f_c(II) = 75.5 MPa). The size range under examination was equal to 1:4 for both Series and, as usual, only a two-dimensional similitude was present, with the thickness of the beams being constant and equal to 127 mm.

The application of the MFSL to the data from Series I (low-strength concrete, LSC) is described in Fig. 10a: the best-fitting values are $\mathcal{G}_F^{\infty}$ = 129.5 N/m and l_{ch} = 104.1 mm respectively, and the correlation coefficient results in R = 0.892. From the value of the internal length l_{ch}, the non-dimensional parameter α = 16.3 is obtained. The application of the MFSL to the data from Series II (high-strength concrete, HSC) is shown in Fig. 10b: in this case, the best-fitting procedure provides $\mathcal{G}_F^{\infty}$ = 160 N/m, l_{ch} = 320.9 mm, α = 50.1 and R = 0.921. In the latter case, the asymptotic fracture energy turns out to be about 130% higher than the smallest specimen's value (68 N/m), and the non-dimensional parameter α results in an anomalously large value with respect to the other cases (where α is generally comprised between 10 and 20).

An interesting comparison can be drawn between the strength and toughness properties of the two Series. While the strength value of Series II is in fact 114% larger than in Series I, a much smaller difference (24%) between the asymptotic fracture energies of the two Series has been detected. This confirms the (relative) increase of brittleness corresponding to the increase of compactness and homogeneity in the microstructure which, in turn, tends to increase the strength value. The transition to a more brittle behavior, in the case of the HSC, can be synthesized by means of Carpinteri's Brittleness Number s [22]: supposing, in fact, that the tensile strength values are equal to one-tenth of the compressive strengths and setting b = 100 mm for both Series, one would obtain $s_{(Series\ I)}$ = 0.00037 and $s_{(Series\ II)}$ = 0.00021, thus concluding that the larger the strength, the larger the brittleness.

An innovative test procedure has been recently developed by Carpinteri and Ferro in order to determine the tensile properties of concrete [23]. Bone-shaped specimens are tested in direct tension, under displacement-controlled loading. The specimens are bounded with stiff plates at their ends, and the reacting section is subjected to tractions always being centered with respect to the progressively-damaged ligament. This is provided by the use of three independent jacks, the first one acting axially and the others on the two principal planes, in order to compensate for the load eccentricities due to the non uniform damage through the reacting ligament. Therefore, no bending moment is present during the loading process. A larger fracture energy, with respect to the three-point bending tests, is obtained: this is due to the (infinite) stiffness of the boundary conditions, which may give rise to the formation of two macrocracks instead of one as in the RILEM test, and to their subsequent bridging, thus resulting in a long-tail softening.

The details of the experimental procedure are exhaustively described in [23]: the maximum aggregate size is d_{max} = 16 mm, and the average compressive strength is equal to 36.9 MPa. A two-dimensional similitude is present, with the thickness t of the "bones" being constantly equal to 100 mm. A 1:8 size interval has been tested, ranging from b = 50 mm to 400 mm, with b being the width at the neck of the specimens.

The application of the MFSL is shown in Fig. 11; the asymptotic fracture energy results in $\mathcal{G}_F^{\infty}$ = 226.4 N/m, and the characteristic internal length l_{ch} = 328.8 mm. On the basis of equation (9), the non-dimensional parameter α results equal to $\alpha = l_{ch} / d_{max}$ = 20.5. The correlation coefficient turns out to be R = 0.864.

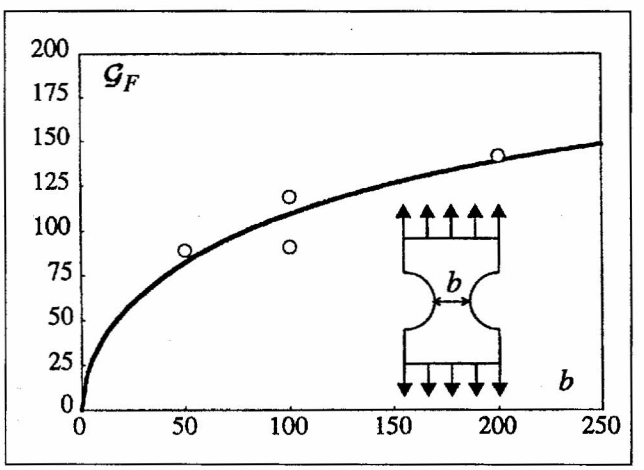

Fig. 11 – Application of the MFSL to the data by Carpinteri and Ferro [23].

5. CONCLUSIONS: DUALITY OF THE MULTIFRACTAL SCALING LAWS FOR STRENGTH AND TOUGHNESS

It is interesting to note the perfect duality existing between the Multifractal Scaling Laws obtained for strength [2] and the toughness of disordered materials. The progressive rarefaction, due to damage, of the resisting ligament, as well as the disordered evolution of the fracture surface, can be modeled by means of fractal domains, with a *lacunar* fractal (with topological dimension smaller than 2) in the case of the ligament and an *invasive* fractal (with topological dimension larger than 2) in the case of the fracture surface, respectively. By applying a Renormalization Group procedure, these hypotheses yield the decrement of nominal tensile strength and the

increment of nominal fracture energy respectively, with increasing structural size.

The multifractal nature of the material microstructure, which has been experimentally detected by the authors [1] and has been indirectly confirmed by the observed trends of the nominal mechanical quantities, provides a transition from disorder to order in the scaling behavior of these quantities, thereby yielding, for strength and toughness respectively, the following Multifractal Scaling Laws:

$$\sigma_u(b) = f_t\left[1 + \frac{l_{ch}}{b}\right]^{1/2} \tag{10a}$$

$$\mathcal{G}_F(b) = \mathcal{G}_F^{\infty}\left[1 + \frac{l_{ch}}{b}\right]^{-1/2} \tag{10b}$$

where the exponent ± 1/2 comes from the (thermodynamic) hypothesis of a Brownian microscopic disorder of the microstructure [17, 18]. It can be observed in equations (10) that the unique difference between the Multifractal Scaling Laws is in the sign of the exponents, connected with the different kind of topology involved in the phenomenon, that defines the asymptotic behavior of the considered mechanical quantity as the structural size tends to zero.

An extensive experimental and statistical investigation is still necessary in order to verify the relationship between the lengths l_{ch} in the two Scaling Laws and in order to confirm the validity of equation (9), which allows connecting such internal lengths to a characteristic granulometric size. Size ranges of more than one order of magnitude should preferably be considered, and various mixtures of concrete should be compared.

ACKNOWLEDGEMENTS

The present research was carried out with the financial support of the Ministry of University and Scientific Research (MURST) and the National Research Council (CNR).

REFERENCES

[1] Carpinteri, A. and Chiaia, B., 'Multifractal nature of concrete fracture surfaces and size effects on nominal fracture energy', *Materials and Structures*, **28** (182) (1995) 435-443.

[2] Carpinteri, A., Chiaia, B. and Ferro, G., 'Size effects on nominal tensile strength of concrete structures: multifractality of material ligaments and dimensional transition from order to disorder', *Materials and Structures*, **28** (180) (1995) 311-317.

[3] Hillerborg, A., Modeer, M. and Petersson, P.E., 'Analysis of crack formation and crack growth in concrete by means of fracture mechanics and finite elements', *Cement and Concrete Research*, **6** (1976) 773-782.

[4] RILEM Technical Committee 50, 'Determination of the fracture energy of mortar and concrete by means of three-point bend tests on notched beams', Draft Recommendation, *Materials and Structures*, **18** (1985) 287-290.

[5] Hillerborg, A., 'Results of three comparative test series for determining the fracture energy $\mathcal{G}_F$ of concrete', *Materials and Structures*, **18** (1985) 407-413.

[6] Swartz, S.E. and Refai, T.M.E., 'Influence of size effects on opening mode fracture parameters for precracked concrete beams in bending', Proceedings of the SEM/RILEM Int. Conf. Fracture of Concrete and Rock (Shah and Swartz eds., Houston, 1987), pp. 403-417.

[7] Wittmann, F.H., Mihashi, H. and Nomura, N., 'Size effect on fracture energy of concrete', *Engineering Fracture Mechanics*, **35** (1990) 107-115.

[8] Hu, X.Z. and Wittmann, F.H., 'Fracture energy and fracture process zone', *Materials and Structures*, **25** (1992) 319-326.

[9] Mai, Y.W. and Cotterell, B., 'Effect of specimen geometry on the essential work of plane stress ductile fracture', *Engineering Fracture Mechanics*, **21** (1985) 123-128.

[10] Guinea, G.V., Planas, J. and Elices, M., 'Measurement of the fracture energy using three-point bend tests: Part 1 –Influence of experimental procedures', *Materials and Structures*, **25** (1992) 212-218.

[11] Planas, J., Elices, M. and Guinea, G.V., 'Measurement of the fracture energy using three-point bend tests: Part 2 –Influence of bulk energy dissipation', *Materials and Structures*, **25** (1992) 305-312.

[12] Elices, M., Guinea, G.V. and Planas, J., 'Measurement of the fracture energy using three-point bend tests: Part 3 –Influence of cutting the P–δ tail', *Materials and Structures*, **25** (1992) 327-334.

[13] Bažant, Z.P. and Kazemi, M.T., 'Size dependence of concrete fracture energy determined by the RILEM work-of-fracture method', *Int. Jour. Fracture*, **51** (1991) 121-138.

[14] Bažant, Z.P., 'Size effect in blunt fracture: concrete, rock, metal', *Journal of Engineering Mechanics*, ASCE, **110** (1984) 518-535.

[15] Karihaloo, B.L. and Nallathambi, P., 'Size-effect prediction from effective crack model for plain concrete', *Materials and Structures*, **23** (1990) 178-185.

[16] Jenq, Y. and Shah, S.P., 'Two-parameter fracture model for concrete', *Jour. Eng. Mech.*, ASCE, **111** (1985) 1227-1241.

[17] Carpinteri, A., 'Scaling laws and renormalization groups for strength and toughness of disordered materials', *International Journal of Solids and Structures*, **31** (1994) 291-302.

[18] Carpinteri, A., 'Fractal nature of material microstructure and size effects on apparent mechanical properties', *Mechanics of Materials*, **18** (1994) 89-101.

[19] Bosco, C. and Iori, I., 'Sulla meccanica della frattura dei laterizi: indagine sperimentale di elementi inflessi ed analisi di parametri caratteristici', *Studi e Ricerche*, **13** (1992) 269-300.

[20] Marquardt, D.W., 'An algorithm for least-squares estimation of nonlinear parameters', *Jour. Soc. Industr. Appl. Math.*, **11** (1963) 431-441.

[21] Perdikaris, P.C. and Romeo, A., 'Effect of size and compressive strength on the fracture energy of plain concrete', Proceedings of the First International Conference on Fracture Mechanics of Concrete Structures, FRAMCOS1, (Bažant ed., Breckenridge, 1992) pp. 550-555.

[22] Carpinteri, A., 'Mechanical Damage and Crack Growth in Concrete: Plastic Collapse to Brittle Fracture', (Martinus Nijhoff Publishers, Dordrecht, 1986).

[23] Carpinteri, A. and Ferro, G., 'Size effects on tensile fracture properties: a unified explanation based on disorder and fractality of concrete microstructure', *Materials and Structures*, **27** (1994) 563-571.